

Selectivity Control of H₂/O₂ Plasma Reaction for Direct Synthesis of High Purity H₂O₂ with Desired Concentration

Yanhui Yi,^a Chao Xu,^b Li Wang,^a Juan Yu,^a Quanren Zhu,^a Shuaiqi Sun,^a Xin Tu,^b Changgong Meng,^c Jialiang Zhang,^d Hongchen Guo^{*a}

a: State Key Laboratory of Fine Chemicals, School of Chemical Engineering, Dalian University of Technology, Dalian 116024, Liaoning, China

b: Department of Electrical Engineering and Electronics, University of Liverpool, Liverpool, L693GJ, U.K.

c: School of Chemistry, Dalian University of Technology, Dalian 116024, Liaoning, China

d: School of Physics and Optoelectronic Engineering, Dalian University of Technology, Dalian 116024, Liaoning, China

* Corresponding author.

Prof. Hongchen Guo.

Tel.: +86 411 84986120;

Fax: +86 411 84986120.

E-mail address: hongchenguo@163.com

ABSTRACT: Low selectivity is one of the key problems which limit the application of plasma in chemical fields. High selectivity and concentration of H₂O₂ are critical in the direct synthesis of H₂O₂. Herein, we report that the selectivity of the H₂/O₂ plasma reaction can be controlled by specific energy input (SEI), i.e. low SEI leads to high H₂O₂ selectivity. When the SEI was fixed at 2.08 J/ml, the H₂O₂ selectivity reached 91% with 17% O₂ conversion, and a H₂O₂ solution with high concentration (90 wt.%) was achieved. Plasma diagnostics and theoretical calculation results indicate that, low SEI results in low electron density, which leads to high H₂O₂ selectivity but low O₂ conversion. Furthermore, the collision cross sections of H₂ and O₂ molecules with electrons indicate that the H₂/O₂ plasma, with average electron energy of 1~1.5 eV, can synthesize H₂O₂ with high selectivity and high O₂ conversion.

Key Words: Plasma Chemistry; Hydrogen Peroxide; Direct Synthesis; Selectivity Control; Electron Density; Average Electron Energy

1 Introduction

Plasma as the fourth state of natural matter has great potential in chemistry, physics and biomedicine [1-4]. During the 1960~80's, chemical synthesis using plasma chemistry was a hot topic[5-8]. In recent years, non-thermal plasma (NTP) has again been adopted by chemists for chemicals conversion [9-11], materials preparation [12-18], and environmental cleanup[19, 20]. Although NTP shows some unique features in the chemical reaction processes mentioned above, low selectivity to the target product is a critical problem researchers have to face, in particular in the synthesis of chemicals. Until now, only a few simple plasma reactions with only one reactant (e.g., acetylene synthesis) or one product (e.g., ozone synthesis) have been applied on industrial scale.

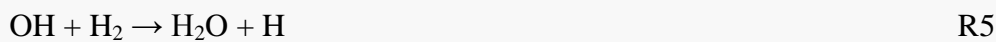
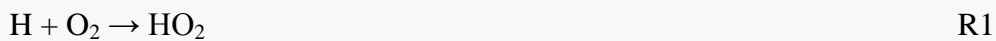
Hydrogen peroxide (H_2O_2), as one of the 100 most important chemicals in the world, has extensive applications [21], such as in paper manufacturing, environmental protection (treatment of waste water and removal of organic pollutants), metallurgy, chemical synthesis (propylene oxide, cyclohexanone oxime, etc), medical treatment (disinfectant), the electronics industry (as a cleaning agent, corrosion inhibitor and as a photoresist removal agent of semiconductor crystal plates in microelectronics, displays and photovoltaics), as well as aerospace (liquid chemical propellant) [22-25]. Industrially, H_2O_2 is almost exclusively produced by a Palladium-catalyzed anthraquinone (AQ) process, where H_2O_2 is synthesized through sequential hydrogenation and oxidation of alkyl anthraquinone [26]. Thus, the AQ process has high safety regarding the non-direct contact between H_2 and O_2 .

However, the emission of exhaust gas (mesitylene isomers), waste water (containing aromatics, 2-ethyl-anthraquinone, tri-octyl phosphate, tert-butyl urea and K_2CO_3 lye) and solid waste (activated alumina) is unacceptable nowadays. In addition, for economic feasibility, the AQ process can only be operated at large-scale, resulting in some security risks in the transportation and storage of concentrated H_2O_2 ; a strict safety policy must therefore be followed.

During the last two decades, the direct synthesis of hydrogen peroxide (DSHP) from molecular H_2 and O_2 over noble metal catalysts, such as Pd [27-30], Au [31-33], Pd-Au [34-38], Pd-Pt [39-40], Pd-Sn [41] and Pt-Au-Pd [42, 43] has attracted much attention. The DSHP is a green and economic process in comparison to the industrial AQ process, and it has great potential to be applied on a small scale, i.e., operated where needed to produce a desired H_2O_2 concentration [44]. However, due to the usage of metal catalysts and organic solvent, it is difficult to get pure H_2O_2 solution directly via the DSHP process; thus some separation and purification units must be employed, which are unfavorable and impractical for small scale application. Furthermore, the side reaction of H_2O_2 hydrogenation occurs on Pd catalysts, which results in a decrease of H_2O_2 concentration. Currently, the highest H_2O_2 concentration obtained by DSHP is still only around ~10 wt.%, which must be improved to make the process feasible (usually about 30 wt.%).

Our previous research has demonstrated that the DSHP could also be realized through a safe H_2/O_2 plasma reaction in a double dielectric barrier discharge (DDBD) reactor [45, 46]. The plasma DSHP is a green gas-phase radical reaction

process and it does not use any catalysts or solvents, thus high purity H₂O₂ could be obtained directly without any purification operations. We also found out that, in the plasma DSHP process, the dissociation of H₂ (driven by electrons through inelastic collision) induced the H₂/O₂ plasma reaction to synthesize H₂O₂ through a chain termination reaction path (R1-R2). Meanwhile, the activation of O₂ (also driven by electrons through inelastic collision) resulted in the formation of H₂O through a chain branching reaction path (R3-R5). Once the O₂ is activated, the by-product H₂O will be easily produced. The difficulty in achieving high selectivity of H₂O₂ therefore lies in activating the H₂ molecule selectively whilst not activating O₂ molecule. In our previous studies, different kinds of DBD reactors were used, but the activation of O₂ could not be inhibited completely. Thus, the optimized H₂O₂ selectivity was nearly 65 % [45, 47, 48], that is, the concentration of H₂O₂ solution obtained by plasma DSHP was about 65 wt.%.



Herein, we report that, in a double dielectric barrier discharge (DDBD) reactor, the selectivity of H₂O₂ in the H₂/O₂ plasma reaction process can be controlled by adjusting the specific energy density (SEI). Lower SEI is favorable to achieve higher H₂O₂ selectivity.

2 Experimental

2.1 Experimental Setup

The experimental setup is shown in Figure 1. The flow of H₂ and O₂ were controlled by mass flow controllers (H₂ 170 ml/min and O₂ 10 ml/min), and the composition of H₂/O₂ mixture was controlled so as to be out of the explosion limit (explosion limit 4%-94%). Before discharge, H₂ and O₂ were mixed homogeneously and passed through the DDBD plasma reactor for about 10 minutes to remove O₂ and N₂ to ensure a safe operating procedure. The temperature of the circulating water was maintained at ca. 2 °C by a refrigeration unit. Then the voltage of the high voltage electrode (HVE) was adjusted to initiate the discharge (High performance computerised plasma and corona discharge experiment generators CTP-2000K). The exhaust gas was analyzed by an on-line gas chromatograph. The H₂O₂ concentration of the collected product solution was determined by iodimetry, then the H₂O₂ selectivity was calculated using formula F2. The discharge voltage, discharge current and power were measured on site by a digital oscilloscope (Tektronix DPO 3012, HV probe Tektronix P6015A, current probe Pearson 6585). The discharge images were taken by a camera (Nikon D50). The optical emission spectra of H₂/O₂ plasma were monitored by a spectrograph (Princeton Instrument SP 2758, 300 G/mm grating, 0.5 s exposure time). When a H₂/O₂ mixture is transformed into a H₂/O₂ DBD plasma, H₂O₂ and H₂O are formed through gas-phase radical reactions and H₂O is the only by-product. The produced H₂O₂ and H₂O will condense on the reactor wall, and then flow into the collector, which is cooled by an ethylene glycol cryogenic

device (-20 °C).

The conversion of O₂ was defined using formula F1, in which the moles of O₂ converted was detected by the gas chromatograph. The selectivity of H₂O₂ was calculated using formula F2, in which the moles of H₂O₂ produced were measured by iodimetry method. Energy consumption was calculated using formula F3, in which the energy consumed was the mathematical product of SEI and total gas flow rate. The SEI was the discharge power divided by total gas flow rate (180 ml/min = 3 ml/s).

$$C_{O_2} = \frac{\text{moles of } O_2 \text{ converted}}{\text{moles of initial } O_2} \times 100\% \quad \text{F1}$$

$$S_{H_2O_2} = \frac{\text{moles of } H_2O_2 \text{ produced}}{\text{moles of } O_2 \text{ converted}} \times 100\% \quad \text{F2}$$

$$E_c = \frac{\text{energy consumed}}{\text{mass of } H_2O_2 \text{ produced}} \quad \text{F3}$$

2.2 Plasma Reactor

The DDBD reactor consisted of a pair of coaxial glass cylinders and two electrodes (Figure 2). The inner cylinder was made of pyrex with an inner diameter of 8.6 mm and an outer diameter of 11mm. The wall of the inner cylinder served as a dielectric barrier for the discharge. The outer cylinder, which had a liquid inlet at the bottom and a liquid outlet at the top, was also made of glass and was used to form an annular gap in between the inner and outer cylinders. The high-voltage electrode (HVE) was a thin pyrex-tube (2.0 mm inner diameter and 4.0 mm outer diameter) fully filled with Nickel powder ($\leq 48 \mu\text{m}$). It was installed in the axis of the cylinders

and connected to the high voltage power supply (AC). The grounding electrode (GE) was an 0.1 wt% NaCl solution, which filled the annular gap of the glass cylinders, and was linked to the grounding wire through a tungsten connection welded across the wall of the outer cylinder. When the reactor was set to work, the aqueous solution of the liquid grounding electrode was recycled so that it served as a cooling agent at the same time. The HV electrode and the grounding electrode formed a cylindrical discharge space, with a length of 250 mm and a volume of 11.375 ml.

2.3 Measurement of H₂O₂ Concentration and Purity

The concentration of H₂O₂ solution produced was measured using an iodimetry method. Firstly, 0.5 g H₂O₂ product was transferred into a volumetric flask (50 ml) using an electronic balance, and then diluted to 50 ml using distilled water. Then 0.2 ml diluted H₂O₂ solution was transferred into a conical flask, before diluting it with 15 ml deionized water. After that, appropriate dilute H₂SO₄ solution was added, along with excess KI powder and 2 drops ammonium molybdate solution (2 wt.%), into the conical flask. This was shaken up and left to stand for ten minutes. The titration operation was then carried out using 0.01 mol/L sodium thiosulfate solution. The H₂O₂ concentration, moles and mass can be calculated based on the reactions R6 and R7. The purity of the produced H₂O₂ solution, i.e. the content of impurities, was analyzed using inductively coupled plasma atomic emission spectroscopy (ICP-AES, Optima 2000 DV, Perkin Elmer).



2.4 Measurement of Electrical Parameters of the H₂/O₂ DBD Plasma

According to the relative dielectric constant of pyrex material and the geometric dimension of the two layer barrier dielectrics in the DDBD reactor, their capacitors have been calculated to be $C_{d1} 9.0265 \times 10^{-11}$ F and $C_{d2} 2.5437 \times 10^{-10}$ F. Thus, the total dielectrics capacitor (C_d) has been calculated to be 6.65×10^{-11} F using formula F4 (series connection).

$$C_d = \frac{C_{d1} \times C_{d2}}{C_{d1} + C_{d2}} \quad \text{F4}$$

The electrical parameter of H₂/O₂ DBD plasma has been measured using the method described in the literature [49]. An external capacitor (C_{ext}) with a capacitance value of 2.28×10^{-8} F has been used as shown in Figure 1. The applied voltage (U_a), external capacitor voltage (U_c) and discharge current can be directly detected by a digital oscilloscope. The dielectric voltage (U_d) can then be calculated using the formula F5. The breakdown voltage, i.e., gas voltage (U_g) can be calculated using the formula F6.

$$U_d = \frac{C_{ext} \times U_c}{C_d} \quad \text{F5}$$

$$U_g = U_a - U_d \quad \text{F6}$$

3 Modeling

3.1 Descriptions of the Simulations

A 0-dimension time-evaluated model was adopted using the software ZDplaskin [50, 51]. We assumed that no surface reactions and recirculation appeared in our

double dielectric barrier discharge (DDBD) reactor so that all species present in the plasma gas satisfy the conditions for solving the Boltzmann Equation F7.

$$\frac{\partial f}{\partial t} + \nu \cdot \nabla f - \frac{e}{m} E \cdot \nabla \nu f = C[f] \quad \text{F7}$$

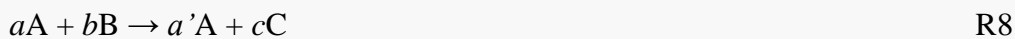
Where E is the electric field, m is the electron mass, f is the electron energy distribution function (EEDF), e is the elementary charge, ν is the average electron velocity and $C[f]$ represents the change rate of f . This simulation can be classified into three main blocks; thirty-six electron-neutral/radical reactions, including momentum transfer, excitations/de-excitations, dissociation and ionization reactions; twenty-four neutral-neutral reactions; five ion-neutral/radical/ion reactions. All simulated species are shown in Table 1. Some other data used in this modeling has been summarized in Supporting Information (Table S1, S2 and S3).

3.2 Physical Model

The time evolution density of species, $N_{i=1\dots i_{\max}}$, can be written as equation F8. The source terms Q_{ij} describe the contribution from each diverse reaction process, $j=1\dots j_{\max}$, defined by user's input file.

$$\frac{d[N_i]}{dt} = \sum_{j=1}^{j_{\max}} Q_{ij}(t) \quad \text{F8}$$

In order to provide a better understanding, an example of the reaction R8 has been provided. The reaction rate can be calculated in equation F9. Therefore, the source terms will be expressed as equation F10, F11 and F12.



$$R = k_j [A]^a [B]^b \quad \text{F9}$$

$$Q_A = (a' - a)R \quad \text{F10}$$

$$Q_B = -bR \quad \text{F11}$$

$$Q_C = cR \quad \text{F12}$$

However, for some temperature-sensitive reactions, the temperature transport is then important (F13).

$$\frac{N_{gas}}{\gamma - 1} \frac{dT_{gas}}{dt} = \sum_{j=1}^{j_{max}} \pm \delta \varepsilon_j \cdot R_j + P_{elast} \cdot [N_e] \quad \text{F13}$$

Here γ is the specific gas heat ratio, $P_{elast} [N_e]$ means the joule heating caused by discharge current, and $\delta \varepsilon_j$ is the energy gap between the initial and final diabatic surfaces of the given reaction step. Additionally, calculations of the rate constants, k_j , are different if electrons are taken into account. For the neutral-neutral reactions, the constants can be obtained from the three-parameter Arrhenius form F14.

$$K_j(T) = A_j T^{B_j} \exp(-E_j/RT) \quad \text{F14}$$

The unit of K_j is in m^3/s . T is gas temperature in Kelvin. The three parameters of A_j , B_j and E_j represent pre-exponential factor, temperature factor, and activation energy, respectively. There has been plenty of research conducted into the synthesis of H_2O_2 , so all parameters used in this work can be found from NIST database.

However, for the electron-impact reactions, a special range of E/n was used to solve the Boltzmann Equation F7 in order to obtain the electron distribution function

and mean electron temperature, while the rate constants for all electron-impact reactions can be calculated by equation F15.

$$k = G \int_0^{\infty} \varepsilon \sigma_k F d\varepsilon \quad \text{F15}$$

Where σ_k is the cross-section of the target particle, F represents the EEDFs, and ε ($\varepsilon = v/G$) is the electron energy in volt ($G = \sqrt{2e/m}$). The maximum value of E/n is observed around 88 Td.

4 Results and Discussion

4.1 H₂/O₂ Plasma Reaction Results

As shown in Table 2, when the SEI increased from 2.08 to 7.09 J/ml, the O₂ conversion increased gradually from 17 % to 99 %; however, the H₂O₂ selectivity decreased gradually from 91% to 20 % and the concentration of H₂O₂ also showed a similar trend with H₂O₂ selectivity. That is, in the case of low SEI, the H₂O₂ could be synthesized with high selectivity, although the O₂ conversion was low. With the increase of SEI, the energy consumption for the production of unit mass of H₂O₂ (Table 2) also increased. At low SEI of 2.08 J/ml, the energy consumption was reduced to 44 kW h/kg_{H₂O₂}, which was lower than the previous result of 53 kW h/kg_{H₂O₂} [46]. The energy consumption reduction could be attributed to the improvement in H₂O₂ selectivity. When the SEI was fixed at 2.08 J/ml, a long-run operation with 500 hours continuous synthesis was conducted, the result of which is shown in Figure 3. It can be seen that the O₂ conversion remained relatively stable whilst the volume of H₂O₂ solution obtained (90 wt.%) increased linearly with reaction time. This means that the H₂/O₂ plasma reaction process can be operated with high stability, which is critical for future practical application.

After the 500 hours reaction, the concentration of the H₂O₂ product obtained was measured to be as high as 90 wt%. Furthermore, the content of impurities in the H₂O₂ product obtained was measured using an inductively coupled plasma atomic emission spectroscopy. The results (Table 3) indicate that the content of inorganic ion impurities were at Grade 2 of the equipment and materials international standards (Table 4), hence it can be used in the electronics industry. Our previous paper reported that Grade 1 electronic H₂O₂ solution could be synthesized by a H₂/O₂ plasma reaction. The reason for improvement of purity could be that the SEI has decreased, and lower SEI means fewer impurities (Zn, As, Mg, Ca and B) are sputtered out of dielectrics by DBD. Generally, at ambient temperature, high concentration H₂O₂ solution readily decomposes. Additionally, some metal ions can also catalyze the decomposition of H₂O₂; thus stabilizers are usually used. However, in this experiment, the 90 wt% H₂O₂ solution can be stored stably without using any stabilizers. The reasons might be, firstly, H₂O₂ solution was stored in a collector (Figure 1) cooled at a low temperature (-20 °C) by an ethylene glycol cryogenic device. Secondly, the content of some metal ions in H₂O₂ solution produced is very low (Table 3) .

Commercially, H₂O₂ is classified by its mass concentration, i.e., 30%, 35%, 50%, 60% and 70%, corresponding to different industrial applications. These commercial H₂O₂ solutions usually contain a small quantity of mechanical impurities, inorganic impurities and organic impurities. However, some high-end applications (electronic industry, medical treatment, food sterilization and aerospace) require a high purity or

high concentration H_2O_2 product. In industry, high purity H_2O_2 (electronic grade or food grade) is produced from the commercial H_2O_2 mentioned above by using a variety of purification methods (distillation, ion exchange resins, membrane separation, supercritical fluid extraction and crystallization). Concentrated H_2O_2 (propellant grade H_2O_2 , higher than 90 wt.%) is usually produced from high purity H_2O_2 through some deep enrichment operations (vacuum distillation and recrystallization operations). These purification and enrichment operations have a huge equipment cost, a long production cycle and consume a copious amount of energy. Therefore, the value and price of H_2O_2 products usually increase exponentially with the concentration and purity of the H_2O_2 solution.

The above experimental results indicate that the selectivity of the H_2/O_2 plasma can be controlled to synthesize high purity and high concentration H_2O_2 directly without any purification or concentration operations. More importantly, through either dilution of 90 wt% H_2O_2 solution or adjusting the input energy density, the concentration of H_2O_2 can be controlled to a desired value for many applications, i.e., paper manufacturing, environment protection, metallurgy, chemical synthesis, medical treatment, electronic industry, as well as aerospace, ranging from dilute to concentrated H_2O_2 solutions.

4.2 Diagnostic of the H_2/O_2 Plasma

As mentioned previously, low reaction selectivity is a key problem of plasma chemical processes. The improvement of H_2O_2 selectivity is also an important issue in the field of H_2O_2 synthesis. Therefore, the control of H_2O_2 selectivity by adjusting SEI, as mentioned above, should be paid enormous attention as it may not only shed

new light on the methodology for the control of plasma chemical reactions, but it may also be significant in H₂O₂ synthesis. In order to understand why the H₂O₂ selectivity can be controlled by SEI, on-site diagnostic studies and theoretical calculation were carried out at different SEI.

The discharge behavior of the H₂/O₂ plasma has been recorded by a camera. The optical images (Figure 4) show that all of the H₂/O₂ plasma exhibited similar diffusive and uninterrupted discharge behavior throughout the discharge zone, just like the behavior of the Townsend discharge. That is, the SEI has little influence on the discharge behavior. However, Figure 4 shows that the luminance of the H₂/O₂ plasma was enhanced with the increase of SEI, which indicates that there may be more active and electronic excited species generated in the H₂/O₂ plasma in the case of higher SEI.

On-site optical emission spectroscopy (OES) has been used to diagnose the active and electronic excited species formed in the H₂/O₂ plasma. As shown in Figure 5a, the OES of the H₂/O₂ plasma was quite complex; two main emission bands in the range of 380-550 nm and 580-650 nm, as well as an intensive emission line at 656.3 nm, were detected. Furthermore, the local enlargement (Figure 5b) shows that two weak emission lines at 777.5 and 844.7 nm were also detected. The above detected five emissions correspond to the decay of H₂ molecule ($a^3\Sigma_g^+ \rightarrow b^3\Sigma_u^+$ and $d^3\Pi_u^+ \rightarrow a^3\Sigma_g^+$), hydrogen atom ($3d^2D \rightarrow 2p^2P^0$) and oxygen atom ($3s^5S^0 \rightarrow 3p^5P$ and $3s^3S^0 \rightarrow 3p^3P$), respectively. It means that both H₂ and O₂ were dissociated in the H₂/O₂ plasma. Figures 5a and 5c show that the emission intensities of the excited H₂,

H and O increase with the increasing of SEI, which indicates more O₂ and H₂ have been activated into active species (H₂^{*}, O₂^{*}, H and O) at higher SEI. Correspondingly, the concentration of active species (H₂^{*}, O₂^{*}, H and O) also increased with SEI. The active oxygen species (O and O₂^{*}) can result in the formation of H₂O through a chain branching reaction path (R3-R5) [45]. This is the reason why the H₂O₂ selectivity decreased with the increasing of SEI.

In atmospheric plasma chemical process, the electron density and average electron energy are the two critical parameters, which usually determine the distribution of active species and subsequently determine the final reaction results. However, they are difficult to measure accurately through experimental methodologies (e.g. Langmuir Probe) because of high deviation caused by high gas density. Fortunately, the variation of the electron density and average electron energy are commonly synchronous with the discharge current and breakdown voltage, respectively. Therefore, an on-site digital phosphor oscilloscope has been used to measure the discharge current and breakdown voltage of the H₂/O₂ plasma with different SEI [47]. The SEI was modulated by varying the applied voltage. However, as shown in Table 5, with increasing SEI, the breakdown voltage (U_g) was nearly stable. That is, the electric field intensity in the discharge region was nearly constant with increasing SEI. So, it can be speculated that the average electron energy in the H₂/O₂ plasma also undergoes little change with the variation of SEI. However, the discharge current increased gradually with an increase in SEI (Table 5), which indicates that the electron density increased gradually with increasing SEI.

4.3 Modeling Results of the H₂/O₂ Plasma

In order to corroborate the above experimental results, theoretical simulations on the H₂/O₂ plasma with different SEI have been calculated using the software ZDplaskin [50, 51]. In the modeling, through solving the Boltzmann Equation F7, the average electron energy and electron density can be calculated. Figure 6 shows that, with the increase of SEI from 2.08 to 7.09 J/ml, the average electron energy was nearly constant, but the electron density increased gradually from 1.54×10^{13} to 4.54×10^{14} cm⁻³. These modeling results (Figure 6) are consistent with the experimental speculation on electron density and average electron energy (Table 5).

The above theoretical simulation results further indicate that the control of H₂O₂ selectivity was achieved through adjusting the electron density of the H₂/O₂ plasma. In plasma chemistry, higher electron density means higher probability of inelastic collisions between an electron and a reactant molecule. At the condition of low SEI, the electron density is low. This means the probability of inelastic collision between the electron and reactant molecule (O₂ and H₂) is also low, which leads to most of O₂ molecules remaining in the ground state. Conversely, at a higher SEI, more O₂ molecules will be activated into active oxygen species (O and O₂*). The active oxygen species (O and O₂*) can result in the formation of H₂O by-product through a chain branching reaction path (R3-R5); however, the ground state oxygen molecule mostly leads to the production of H₂O₂ through a chain termination reaction path (R1-R2) [45]. Therefore, low SEI, i.e., low electron density H₂/O₂ plasma, can synthesize H₂O₂ with high selectivity. However, low electron density will also result

in low O₂ conversion and low H₂O₂ yield.

4.4 Method for Future Improvement

The above results have demonstrated that, in order to get high H₂O₂ selectivity and high H₂O₂ yield simultaneously, the electron density of H₂/O₂ plasma must be increased, but the activation of O₂ must be avoided. The inelastic collision cross sections of H₂ [52-57] and O₂ [58-63] molecules with an electron, summarized in Figure 7 (the detail information is shown in supporting information, Figure S1), are vital for achieving this goal. In plasma, higher collision cross sections have higher probability to induce inelastic collision between particles and electrons, which results in activation of the reactant molecule. Figure 7 shows that, when the electron energy is in the range of 0~10 eV, the electrons can activate the H₂ molecule; however, only the electrons with energy in the range of 0.5~1 or 1.5~10 eV can activate the O₂ molecule. In other words, the electrons with energy between 1~1.5 eV can activate H₂ but cannot activate O₂. This result suggests that further study into the H₂/O₂ plasma reaction for the synthesis of H₂O₂ should be focused on controlling the average electron energy in the range of 1~1.5 eV. However, because the electron energy distribution in plasma is statistical (usually Maxwell distribution), the production of electrons with energy outside the range of 1~1.5 eV is inevitable. So, control of average electron energy may be beneficial for the enhancement of H₂O₂ selectivity but complete inhibition of H₂O formation is not possible. In other words, when the average electron energy is controlled in the range of 1~1.5 eV, the chain branching reaction path (R3-R5) to form H₂O by-product can be inhibited partially,

thus higher H₂O₂ selectivity and higher H₂O₂ yield can be obtained simultaneously at higher SEI.

5 Conclusions

In summary, the selectivity of H₂O₂ in the H₂/O₂ plasma reaction process can be effectively controlled by controlling the SEI: The higher the SEI, the lower the H₂O₂ selectivity. Plasma diagnostics and theoretical calculation results indicate that low electron density H₂/O₂ plasma is the critical factor for obtaining high selectivity. When the SEI was fixed at 2.08 J/ml, 500 hours continuous operation was carried out with high stability. The H₂O₂ selectivity reached 91 % and the H₂O₂ product obtained was high purity (electronic grade), producing concentrated H₂O₂ solution (90 wt%). However, low SEI leads to low O₂ conversion and low H₂O₂ yield. In the future, if the average electron energy of H₂/O₂ plasma could be controlled in the range of 1~1.5 eV, higher H₂O₂ selectivity and higher H₂O₂ yield could be achieved simultaneously at higher SEI.

These results provide the idea that, by combining a H₂/O₂ plasma experimental setup with a water electrolysis device, a H₂O₂ generator can be designed to produce high purity H₂O₂ directly from H₂O. Furthermore, only consuming electrical energy, this H₂O₂ generator can synthesize H₂O₂ with a desired concentration ranging from dilute to concentrated H₂O₂ solution, which has broad applications, i.e., paper manufacturing, environment protection, metallurgy, chemical synthesis, medical treatment, electronic industry, as well as aerospace. However, more studies need to be done to improve H₂O₂ productivity and decrease the energy consumption.

In addition, through analyzing the collision cross section of reactants with an electron and adjusting the electron energy distribution, the selectivity of some complex plasma reaction systems (various reactants and products) could be controlled in theory and practical applications.

Acknowledgements

We acknowledge the financial support from Dalian University of Technology [DUT1RC(3)022], Natural Science Foundation of China [20233050 and 21503032] and China Postdoctoral Science Foundation [2015M580220 and 2016T90217]. We also acknowledge Miss Bryony Ashford for help on English Language.

Notation

SEI = specific energy input

NTP = non-thermal plasma

H₂O₂ = hydrogen peroxide

AQ = anthraquinone

DSHP = direct synthesis of hydrogen peroxide

DDBD = double dielectric barrier discharge

DBD = dielectric barrier discharge

HVE = high voltage electrode

AC = alternating current

GE = grounding electrode

C_d = dielectrics capacitor

U_a = applied voltage

U_c = external capacitor voltage

U_d = dielectric voltage

U_g = gas voltage = breakdown voltage

BE = boltzmann equation

EEDF = electron energy distribution function

OES = optical emission spectroscopy

References

- [1] Neyts EC, Ostrikov KK, Sunkara MK, Bogaerts A. Plasma Catalysis: Synergistic Effects at the Nanoscale. *Chem. Rev.* **2015**; *115*: 13408-13446.
- [2] Kong MG, Kroesen G, Morfill G, Nosenko T, Shimizu T, Dijk J, Zimmermann JL. Plasma medicine: an introductory review. *New J. Phys.* **2009**; *11*: 115012-115047.
- [3] Samukawa S, Hori M, Rauf S, Tachibana K, Bruggeman P, Kroesen G, Whitehead JC, Murphy AB, Gutsol AF, Starikovskaia S, Kortshagen U, Boeuf J, Sommerer TJ, Kushner MJ, Czarnetzki U, Mason N. The 2012 Plasma Roadmap. *J. Phys. D: Appl. Phys.* **2012**; *45*: 253001-253037.
- [4] Attri P, Arora B, Choi EH. Utility of plasma: a new road from physics to chemistry. *RSC Adv.* **2013**; *3*: 12540-12567.
- [5] Devins JC, Burton M. Formation of Hydrazine in Electric Discharge Decomposition of Ammonia. *J. Am. Chem. Soc.* **1954**; *76*: 2618-2626.
- [6] Spedding PL. Chemical Synthesis by Gas-phase Discharge. *Nature* **1967**; *214*: 124-126.
- [7] Suhr H, Weiss RI. Single-Step Synthesis of Biphenylene from 9-Fluorenone in a Discharge Plasma. *Angew. Chem. Int. Ed.* **1970**; *9*: 312.
- [8] Suhr H. Organic Synthesis in the Plasma of Glow Discharges and Their Preparative Application. *Angew. Chem. Int. Ed.* **1972**; *11*: 781-792.
- [9] Na N, Xia Y, Zhu Z, Zhang X, Cooks RG. Birch Reduction of Benzene in a Low-Temperature Plasma. *Angew. Chem. Int. Ed.* **2009**; *48*: 2017-2019.
- [10] Sentek J, Krawczyk K, Młotek M, Kalczyńska M, Kroker T, Kolb T, Schenk A, Gericke K, Schmidt-Szałowski K. Plasma-catalytic methane conversion with carbon dioxide in dielectric

barrier discharges. *Appl. Catal. B: Environ.* **2010**; *94*: 19-26.

[11] Zhang J, Yuan Q, Zhang J, Li T, Guo H. Direct synthesis of ethylene glycol from methanol by dielectric barrier discharge. *Chem. Commun.* **2013**; *49*: 10106-10108.

[12] Munir ZA, Anselmi-Tamburini U, Ohyanagi M. The effect of electric field and pressure on the synthesis and consolidation of materials: A review of the spark plasma sintering method. *J. Mater. Sci.* **2006**; *41*: 763-777.

[13] Chu W, Wang L, Chernavskii PA, Khodakov AY. Glow-Discharge Plasma-Assisted Design of Cobalt Catalysts for Fischer-Tropsch Synthesis. *Angew. Chem. Int. Ed.* **2008**; *47*: 5052-5055.

[14] Wang A, Qin M, Guan J, Wang L, Guo H, Li X, Wang Y, Prins R, Hu Y. The Synthesis of Metal Phosphides: Reduction of Oxide Precursors in a Hydrogen Plasma. *Angew. Chem. Int. Ed.* **2008**; *47*: 6052-6054.

[15] Gupta A, Swihart MT, Wiggers H. Luminescent Colloidal Dispersion of Silicon Quantum Dots from Microwave Plasma Synthesis: Exploring the Photoluminescence Behavior Across the Visible Spectrum. *Adv. Func. Mater.* **2009**; *19*: 696-703.

[16] Lin PA, Sankaran RM. Plasma-Assisted Dissociation of Organometallic Vapors for Continuous, Gas-Phase Preparation of Multimetallic Nanoparticles. *Angew. Chem. Int. Ed.* **2011**; *50*: 10953-10956.

[17] Morrish R, Silverstein R, Wolden CA. Synthesis of Stoichiometric FeS₂ through Plasma-Assisted Sulfurization of Fe₂O₃ Nanorods. *J. Am. Chem. Soc.* **2012**; *134*: 17854-17857.

[18] Moon J, An J, Sim U, Cho S, Kang JH, Chung C, Seo J, Lee J, Nam KT, Hong BH. One-Step Synthesis of N-Doped Graphene Quantum Sheets from Monolayer Graphene by Nitrogen Plasma. *Adv. Mater.* **2014**; *26*: 3501-3505.

[19] Durme JV, Dewulf J, Leys C, Langenhove HV. Combining non-thermal plasma with heterogeneous catalysis in waste gas treatment: A review. *Appl. Catal. B: Environ.* **2008**; *78*: 324-333.

[20] Chen HL, Lee HM, Chen SH, Chang MB, Yu SJ, Li SN. Removal of Volatile Organic Compounds by Single-Stage and Two-Stage Plasma Catalysis Systems: A Review of the Performance Enhancement Mechanisms, Current Status, and Suitable Applications. *Environ. Sci. Technol.* **2009**; *43*: 2216-2227.

- [21] R. L. Myers, *The 100 most important chemical compounds a reference guide*. Greenwood Publishing Group: Westport CT, **2007**.
- [22] Kamata K, Yonehara K, Sumida Y, Yamaguchi K, Hikichi S, Mizuno N. Efficient Epoxidation of Olefins with $\geq 99\%$ Selectivity and Use of Hydrogen Peroxide. *Science* **2003**; *300*: 964-966.
- [23] Lane BS, Burgess K. Metal-Catalyzed Epoxidations of Alkenes with Hydrogen Peroxide. *Chem. Rev.* **2003**; *103*: 2457-2473.
- [24] Hage R, Lienke A. Applications of Transition-Metal Catalysts to Textile and Wood-Pulp Bleaching. *Angew. Chem. Int. Ed.* **2006**; *45*: 206-222.
- [25] Yi Y, Wang L, Li G, Guo H. A review on research progress in the direct synthesis of hydrogen peroxide from hydrogen and oxygen: noble-metal catalytic method, fuel-cell method and plasma method. *Catal. Sci. Technol.* **2016**; *6*: 1593-1610.
- [26] Campos-Martin JM, Blanco-Brieva G, Fierro JLG. Hydrogen peroxide synthesis: an outlook beyond the anthraquinone process. *Angew. Chem. Int. Ed.* **2006**; *45*: 6962-6984.
- [27] Choudhary VR, Gaikwad AG, Sansare SD. Nonhazardous direct oxidation of hydrogen to hydrogen peroxide using a novel membrane catalyst. *Angew. Chem. Int. Ed.* **2001**; *40*: 1776-1779.
- [28] Dissanayake DP, Lunsford JH. The direct formation of H₂O₂ from H₂ and O₂ over colloidal palladium. *J. Catal.* **2003**; *214*: 113-120.
- [29] Landon P, Collier PJ, Carley AF, Chadwick D, Papworth AJ, Burrows A, Kiely CJ, Hutchings GJ. Direct synthesis of hydrogen peroxide from H₂ and O₂ using Pd and Au catalysts. *Phys. Chem. Chem. Phys.* **2003**; *5*: 1917-1923.
- [30] Liu Q, Bauer JC, Schaak RE, Lunsford JH. Supported palladium nanoparticles: an efficient catalyst for the direct formation of H₂O₂ from H₂ and O₂. *Angew. Chem. Int. Ed.* **2008**; *47*: 6221-6224.
- [31] Landon P, Collier PJ, Papworth AJ, Kiely CJ, Hutchings GJ. Direct formation of hydrogen peroxide from H₂/O₂ using a gold catalyst. *Chem. Commun.* **2002**; 2058-2059.
- [32] Li G, Edwards J, Carley AF, Hutchings GJ. Direct synthesis of hydrogen peroxide from H₂ and O₂ and in situ oxidation using zeolite-supported catalysts. *Catal. Commun.* **2007**; *8*: 247-250.

- [33] Ouyang L, Tan L, Xu J, Tian P, Da G, Yang X, Chen D, Tang F, Han Y. Functionalized silica nanorattles hosting Au nanocatalyst for direct synthesis of H₂O₂. *Catal. Today* **2015**; *248*: 28-34.
- [34] Edwards JK, Hutchings GJ. Palladium and gold-palladium catalysts for the direct synthesis of hydrogen peroxide. *Angew. Chem. Int. Ed.* **2008**; *47*: 9192-9198.
- [35] Edwards JK, Ntainjua E, Carley AF, Herzing AA, Kiely CJ, Hutchings GJ. Direct synthesis of H₂O₂ from H₂ and O₂ over gold, palladium, and gold-palladium catalysts supported on acid-pretreated TiO₂. *Angew. Chem. Int. Ed.* **2009**; *48*: 8512-8515.
- [36] Edwards JK, Solsona B, Ntainjua E, Carley AF, Herzing AA, Kiely CJ, Hutchings GJ. Switching off hydrogen peroxide hydrogenation in the direct synthesis process. *Science* **2009**; *323*: 1037-1041.
- [37] Freakley SJ, Lewis RJ, Morgan DJ, Edwards JK, Hutchings GJ. Direct synthesis of hydrogen peroxide using Au-Pd supported and ion-exchanged heteropolyacids precipitated with various metal ions. *Catal. Today* **2015**; *248*: 10-17.
- [38] Menegazzo F, Manzoli M, Signoretto M, Pinna F, Strukul G. H₂O₂ direct synthesis under mild conditions on Pd-Au samples: effect of the morphology and of the composition of the metallic phase. *Catal. Today* **2015**; *248*: 18-27.
- [39] Liu Q, Bauer JC, Schaak RE, Lunsford JH. Direct synthesis of H₂O₂ from H₂ and O₂ over Pd-Pt/SiO₂ bimetallic catalysts in a H₂SO₄/ethanol system. *Appl. Catal. A: Gen.* **2008**; *339*: 130-136.
- [40] Xu J, Ouyang L, Da G, Song Q, Yang X, Han Y. Pt promotional effects on Pd-Pt alloy catalysts for hydrogen peroxide synthesis directly from hydrogen and oxygen. *J. Catal.* **2012**; *285*: 74-82.
- [41] Freakley SJ, He Q, Harry JH, Lu L, Crole DA, Morgan DJ, Ntainjua E, Edwards JK, Carley AF, Borisevich AY, Kiely CJ, Hutchings GJ. *Science* **2016**; *351*: 965-968.
- [42] Edwards JK, Pritchard J, Lu L, Piccinini M, Shaw G, Carley AF, Morgan DJ, Kiely CJ, Hutchings GJ. The direct synthesis of hydrogen peroxide using platinum-promoted gold-palladium catalysts. *Angew. Chem. Int. Ed.* **2014**; *53*: 2381-2384.
- [43] Edwards JK, Pritchard J, Miedziak PJ, Piccinini M, Carley AF, He Q, Kiely CJ, Hutchings

GJ. The direct synthesis of hydrogen peroxide using platinum promoted gold-palladium catalysts. *Catal. Sci. Technol.* **2014**; 4: 3244-3250.

[44] Freakley SJ, Piccinini M, Edwards JK, Ntainjua E, Moulijn JA, Hutchings GJ. Effect of reaction conditions on the direct synthesis of hydrogen peroxide with a AuPd/TiO₂ catalyst in a flow reactor. *ACS Catal.* **2013**; 3: 487-501.

[45] Yi Y, Zhou J, Guo H, Zhao J, Su J, Wang L, Wang X, Gong W. Safe direct synthesis of high purity H₂O₂ through a H₂/O₂ plasma reaction. *Angew. Chem. Int. Ed.* **2013**; 52: 8446-8449.

[46] Yi Y, Zhou J, Gao T, Zhang J, Guo H. Continuous and scale-up synthesis of high purity H₂O₂ by safe gas-phase H₂/O₂ plasma reaction. *AIChE. J.* **2014**; 60: 415-419.

[47] Zhou J, Guo H, Wang X, Guo M, Zhao J, Chen L, Gong W. Direct and continuous synthesis of concentrated hydrogen peroxide by the gaseous reaction of H₂/O₂ non-equilibrium plasma. *Chem. Comm.* 2005; 1631-1633.

[48] Zhao, J, Zhou J, Su J, Guo, H, Wang X, Gong W. Propene Epoxidation with In-Site H₂O₂ produced by H₂/O₂ Non-Equilibrium Plasma. *AIChE. J.* 2007; 53: 3204-3209.

[49] Tu X, Gallon HJ, Twigg MV, Gorry PA, Whitehead JC. Dry reforming of methane over a Ni/Al₂O₃ catalyst in a coaxial dielectric barrier discharge reactor. *J. Phys. D: Appl. Phys.* **2011**; 44: 274007-274016.

[50] Snoeckx R, Alerts R, Tu X, Bogaerts A. Plasma-Based Dry Reforming: A Computational Study Ranging from the Nanoseconds to Seconds Time Scale. *J. Phys. Chem. C* 2013; 117: 4957-4970.

[51] Pancheshnyi S, Eismann B, Hagelaar G. J. M., Pitchford L. C. Computer code ZDPlasKin, <http://www.zdplaskin.laplace.univ-tlse.fr>, University of Toulouse, LAPLACE, CNRS-UPS-INP, Toulouse, France, 2008.

[52] Corrigan SJB. Dissociation of molecular hydrogen by electron impact. *J. Chem Phys.* **1965**; 43: 4381-4386.

[53] Stibbe DT, Tennyson J. Near-threshold electron impact dissociation of H₂ within the adiabatic nuclei approximation. *New J. Phys.* **1998**;1: 2.1-2.9.

[54] Celiberto R, Janev RK, Laricchiuta A, Capitelli M, Wadehra JM, Atems DE. Cross section data for electron-impact inelastic processes of vibrationally excited molecules of hydrogen and

its isotopes. *Atom. Data Nucl. Data Tab.* **2001**; 77: 161-213.

[55] Laricchiuta A, Celiberto R, Janev RK. Electron-impact-induced allowed transitions between triplet states of H₂. *Phys. Rev. A* **2004**; 69: 022706.

[56] Itikawa Y, Mason N. Rotational excitation of molecules by electron collisions. *Phys. Rep.* 2005; 414: 1-41.

[57] Horacek J, Cizek M, Houfek K, Kolorenc P, Domcke W. Dissociative electron attachment and vibrational excitation of H₂ by low-energy electrons: calculations based on an improved nonlocal resonance model. II. vibrational excitation. *Phys. Rev. A* **2006**; 73: 022701.

[58] Eliasson B, Kogelschatz U. Electron impact dissociation in oxygen. *J. Phys. B: At. Mol. Opt. Phys.* **1986**; 19: 1241-1247.

[59] Cosby PC. Electron-impact dissociation of oxygen. *J. Chem. Phys.* **1993**; 98: 9560-9569.

[60] Allan M. Measurement of absolute differential cross sections for vibrational excitation of O₂ by electron impact. *J. Phys. B: At. Mol. Opt. Phys.* **1995**; 28: 5163-5175.

[61] Allan M. Experimental differential cross sections for the electron impact excitation of the a ¹Ag, b ¹Xi, and the 6 eV states of O₂. *J. Phys. B: At. Mol. Opt. Phys.* **1995**; 28: 4329-4345.

[62] Noble CJ, Higgins K, Woste G, Duddy P, Burke PG, Teubner P, Middleton AG, Brunger MJ. Resonant mechanisms in the vibrational excitation of ground state O₂. *Phys. Rev. Lett.* **1996**; 76: 3534-3537.

[63] Tashiro M, Morokuma K, Tennyson J. R-matrix calculation of electron collisions with electronically excited O₂ molecules. *Phys. Rev. A* **2006**; 73: 052707.

Figure Captions

Fig. 1 – Schematic diagram of experimental setup for direct synthesis of H_2O_2 through H_2/O_2 plasma

Fig. 2 – Schematic structure of the DDBD reactor

Fig. 3 – O_2 conversion and H_2O_2 product solution volume VS. reaction time during the 500 h continuous operation. The left inset is the discharge photo and the right inset is the photo of the H_2O_2 production. (2.08 J/ml SEI, 12 kHz discharge frequency, 1 atm, 10 ml/min O_2 , 170 ml/min H_2)

Fig. 4 – Optical images of the H_2/O_2 DBD plasma at different specific energy input. (0.5 s exposure time, 12 kHz discharge frequency, 1 atm, 10 ml/min O_2 , 170 ml/min H_2).

Fig. 5 – a) OES of the H_2/O_2 DBD plasma with different specific energy input; b) the local enlargement of a); c) OES intensity of H and O atomic lines in the H_2/O_2 DBD plasma with different specific energy input. (300 g/mm grating, 0.5 s exposure time, 12 kHz discharge frequency, 1 atm, 10 ml/min O_2 , 170 ml/min H_2)

Fig. 6 – Electron density and average electron energy of H_2/O_2 plasma as a function of specific energy input simulated using ZDplaskin software.

Fig. 7 – Inelastic collision cross sections of H₂ and O₂ molecule with electron in the energy range of 0~10 eV.

Table 1 – Summary of all ground-state species included in the model.

Table 2 – H₂O₂ synthesis with varying specific energy input in a DDBD reactor.

Table 3 – Impurity content of the H₂O₂ solution obtained in the 500 h continuous operation and the electronic grade H₂O₂ of SEMI Standards (Unite: ppb).

Table 4 – Requirements for electronic grade hydrogen peroxide according to SEMI Standards (SEMI Document C30-1110, 2010).

Table 5 – Electrical parameters of the H₂/O₂ DBD plasma with different specific energy input.